DISSIMILARITIES BETWEEN NUSSELT NUMBER AND TURBULENT KINETIC ENERGY IN DUCTS OF VARYING CROSS SECTION

Edimilson J. Braga
Marcelo J.S. de Lemos
Departamento de Energia - IEME
Instituto Tecnológico de Aeronáutica - ITA
12228-900 – São José dos Campos, SP, Brasil - E-mail: delemos@mec.ita.br

Abstract

This paper presents numerical simulation for turbulent flow in ducts of varying cross section. Dissimilarities between Nusselt number and turbulent kinetic energy are investigated. A marching-forward numerical integration technique is used to sweep the computational domain. Cases of gradual enlargements or contractions in ducts with sinusoidal walls are calculated. Turbulence is handled with the standard isotropic k-ε model. Results show that, within contractions, turbulence is damped whereas, in diffusers, the valued of k is increased also, in contracting ducts, while turbulence is damped, the turbulent Nusselt number increases. Along enlargements, overall turbulent heat transfer is damped.

Keywords: Turbulent, Heat Transfer, Convergent-Divergent Channel

1. INTRODUCTION

Flow passages with contractions and enlargements are commonly found in a number of engineering equipment. Accurate determination of turbulent kinetic energy values and heat transfer rates in such devices contributes to efficiency increase, optimal design parameters and, ultimately, reduction of cost-benefit relationship. Experimental work published on turbulent flows deals, in its majority, with sudden expansion flow into a stagnant surrounding (Buresti *et al*, 1998) or within a confining duct (Park and Chen, 1989. In all of the above, recirculating flow due to abrupt expansion precludes the use of the mathematical treatment below, which in contrast, is based on a marching-forward technique (Patankar, 1988). The compilation work of Spencer *et al*, 1995, seems to be the only available experimental data bank for turbulent flow within contractions and diffusers. Therein, experimental data from 11 institutions around the world, taken for flow of air and water in contraction and diffuser, were compared with each other and with computational results using commercial CFD codes. The authors conclude that, “numerical simulation of turbulent flow through simple pipe components cannot be achieved with the commercial programs available”.

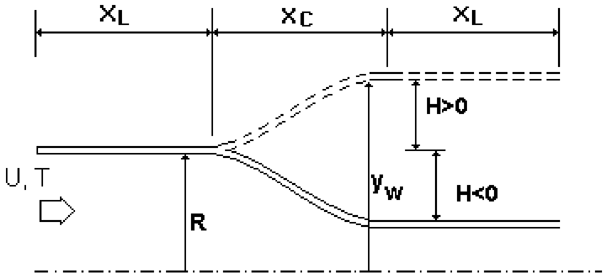

Figure 1 - Notation for general conical ducts with diverging (H>0) and converging (H<0) walls of sinusoidal shape.

Table 1 – Input data for geometry of Figure 1

	Div	Conv
Maximum H/D	+0.4	-0.4
X_L/D	100	
X_C/D	25	

As a consequence, the use of numerical tools for quick analysis of simple engineering flows, instead of using memory demanding CFD codes, has motivated many research efforts recently. If no back flow is in order, marching-forward techniques, implemented along with isotropic turbulence models, provide an economical means for engineering analysis with PC-based workstations.

Following this path, the work of Matsumoto and de Lemos, 1990, presented results for the developing *time-averaged* and *turbulent* fields in a coaxial jet along a circular duct of constant area. Later, de Lemos and Milan, 1997, extended their calculations to flow in long ducts through varying cross sections. De Lemos and Braga (1998) further considered coaxial jets with *higher* ($U_e>U_i$) and *lower* ($U_e<U_i$) annular velocity in *diverging* ($H>0$) and *converging* ($H<0$) ducts of the shape shown in Figure 1. Similar results for ducts with plane walls have also been documented (Braga and de Lemos, 1999a). Experimentally observed turbulence damping in contractions and corresponding enhancement in diffusers, reported in detail by Spencer *et al*, 1995, was correctly simulated.

Heat transfer analysis followed with the work of de Lemos and Braga, 1999b, who reported Nusselt numbers and turbulent kinetic energy in planar diffusers and contractions therein, flow and heat transfer properties of coaxial jets, with higher inner velocity ($U_i>U_e$) and temperature ($T_i>T_e$), were predicted. Interesting dissimilarity between Nusselt number and turbulent kinetic energy was calculated and discussed upon. While turbulence was damped along accelerating flows (contractions), heat transfer was increased by a fair amount.

This opposing behavior is herein further investigated. The present contribution discuss the problem of dissimilarities between Nusselt number and turbulent kinetic energy in ducts of sinusoidal walls with an increase of up to 40% of the initial cross-sectional area (see Fig. 1).

2. ANALYSIS AND NUMERICS

2.1 Governing equations

The equations of continuity of mass, *x*-momentum and energy for a two-dimensional, source-free, low speed, planar/axi-symmetric turbulent mixing layer can be written as,

$$\frac{\partial\ (y^{\eta}\rho u)}{\partial x}+\frac{\partial\,(y^{\eta}\rho v)}{\partial y}=0 \tag{1}$$

$$\rho u \frac{\partial u}{\partial x} + \rho v \frac{\partial u}{\partial y} = - \frac{\partial P}{\partial x} + \frac{1}{y^{\eta}} \frac{\partial}{\partial y} \left[y^{\eta} \; \mu_{eff} \frac{\partial u}{\partial y} \right] \tag{2}$$

$$\rho u \frac{\partial T}{\partial x} + \rho v \frac{\partial T}{\partial y} = \frac{1}{y^{\eta}} \frac{\partial}{\partial y} \left[y^{\eta} \; \Gamma_{eff}^{T} \frac{\partial T}{\partial y} \right] \tag{3}$$

In (1)-(2)-(3) *u*, *v* are the velocity components in the axial and transverse direction, respectively, *T* is the temperature, ρ the fluid density, *P* the static pressure, and μ_{eff}, Γ_{eff}^{T} the coefficients of turbulent exchange given as $\mu_{eff} = \mu_t + \mu$ and $\Gamma_{eff}^{T} = \mu_t / \sigma_T + \mu / \mathrm{Pr}$, respectively. Also, μ is the molecular viscosity, Pr the fluid Prandtl number and μ_t and σ_T the turbulent viscosity and the Prandtl/Schmidt number, respectively. As usual, equations (1)-(2)-(3) are written in a compact notation embracing planar (η=0) and axi-symmetric (η=1) cases.

2.2 Turbulence model

The turbulence model *k*-ε of Jones and Launder, 1972, has been used in the literature in a number of publications. In this approach, the turbulent viscosity mentioned above is calculated as $\mu_t = \rho c_\mu k^2 / \varepsilon$ where c_μ is a constant. Here, as done in de Lemos and Braga, 1999b, only the case involving flow regions of high local Reynolds numbers are considered (Launder and Spalding, 1974). With this, transport equations for *k* and ε can be written as,

$$\rho u \frac{\partial \phi}{\partial x} + \rho v \frac{\partial \phi}{\partial y} = \frac{1}{y^{\eta}} \frac{\partial}{\partial y} \left[y^{\eta} \; \Gamma_{\phi} \frac{\partial \phi}{\partial y} \right] + S_{\phi} \tag{4}$$

In (4) ϕ stands for *k* or ε. The diffusion coefficients are given by $\Gamma_{eff}^{k} = \mu + \mu_t / \sigma_k$ and $\Gamma_{eff}^{\varepsilon} = \mu + \mu_t / \sigma_\varepsilon$ where the σ's are the turbulent Prandtl/Schmidt numbers for *k* and ε, respectively. The last terms in **(4)** are known as "source" terms and are given by $S_k = \rho (P_k - \varepsilon)$ and $S_\varepsilon = \rho \,\varepsilon/k \,(c_1 P_k - c_2 \varepsilon)$, being c_1=1.47, c_2=1.92 and c_μ=0.09. The production term reads $P_k = \mu_t / \rho \; (\partial U / \partial y)^2$.

2.3 Boundary conditions and Computational Details.

The numerical approach adopted here and in de Lemos and Braga, 1999b, is the parabolic solver technique of Patankar (1972, 1988). For clarity, it is reviewed below.

Inlet flows are given a uniform distribution. For temperature, constant value of *T* prevails over the inlet. Also, the values of *k* and ε at entrance were given by $k_{in} = 10^{-3} U_m$ and $\varepsilon_{in} = k_{in}^{3/2} / K y'$ where U_m is the overall mean velocity, K is the von Kármán constant (K=0.4) and *y*' the distance to the wall. For the centerline (*y*=0) the symmetry condition is implemented for all dependent variables ϕ=*U*, *T*, *k* and ε as $\left.\partial \phi / \partial y\right)_{y=0} = 0$. Wall proximity is handled with the **Wall Function** approach (Launder and Spalding, 1972, 1974), giving for the wall shear stress,

$$\tau_w = \left(U_N \rho c_\mu^{1/4} k_N^{1/2} \right) \Bigg/ \frac{1}{K} \ln \left[E \, y_N \frac{\rho (c_\mu^{1/2} k_N)^{1/2}}{\mu} \right] \tag{5}$$

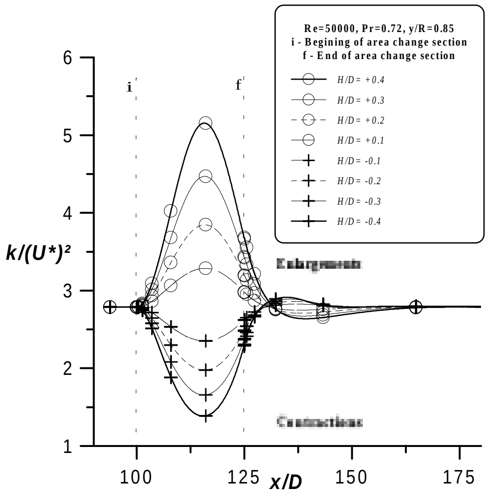

Figure 2 – Development of k/U^{*2} close to the wall for contractions and enlargements

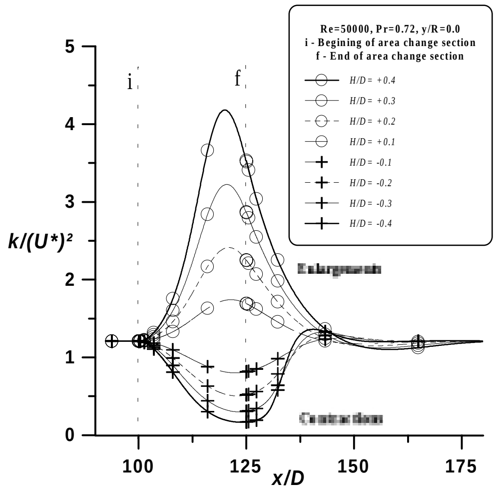

Figure 3 – Development of k/U^{*2} at the duct centerline for contractions and enlargements

Where E is a constant. In (5) the subscript "N" identifies the grid point closest to the wall. In that region, the use of the **Wall Function** associated with the assumption of "<u>local equilibrium</u>" for turbulence ($P_k=\varepsilon$) gives $k_N = \tau_w / \left(\rho\, c_\mu\right)^{1/2}$ *and* $\varepsilon_N = k_N^{3/2} / \mathrm{K}\, y_N$. Rewriting (5) in the form $\tau_w = \lambda\mu(\partial U/\partial y)$ gives further,

$$\lambda = \begin{cases} 1 \quad \text{for laminar flow} \\ \dfrac{\mathrm{K}\, y_N \dfrac{\rho (c_\mu^{1/2} k_N)^{1/2}}{\mu}}{\ln\left[E y_N \dfrac{\rho (c_\mu^{1/2} k_N)^{1/2}}{\mu} \right]} \text{ for turbulent flow} \end{cases} \tag{6}$$

For temperature, the **Wall Law** is given by,

$$T^+ = (T_N - T_w)\rho c_p\, c_\mu^{1/4} k_N^{1/2} / q_w = \frac{Pr_t}{\mathrm{K}} \ln\left[E\, y_N \frac{\mu (c_\mu^{1/2} k_N)^{1/2}}{\rho} \right] + 12.5\, Pr^{2/3} + 2.12\, Pr - c_q \tag{7}$$

where the last term in (**7**) fits experimental data and has been proposed by Kader and Yaglom, 1972. It reads $c_q = 5.3$ for Pr<0.5 and $c_q = 1.5$ for Pr≥0.5. Either case, constant T_w or constant q_w, is analyzed with (**7**). The wall heat flux can be further given after rearranging (**7**) in the form $q_w = -\lambda_T \dfrac{\mu c_p}{Pr} \dfrac{\partial T}{\partial y}$ where;

$$\lambda_T = \begin{cases} 1 \quad \text{for laminar flow} \\ \dfrac{\mathrm{K}\, y_N \dfrac{\rho (c_\mu^{1/2} k_N)^{1/2}}{\mu}\; Pr}{\left(\sigma_T \ln\left[E y_N \dfrac{\rho (c_\mu^{1/2} k_N)^{1/2}}{\mu} \right] + c_q^* \mathrm{K} \right)} \text{ for turbulent flow} \end{cases} \tag{8}$$

with $c_q^* = 12.5\, Pr^{2/3} + 2.12\, Pr - c_q$.

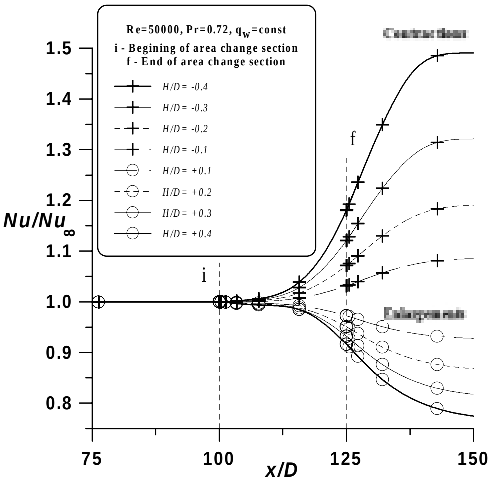

Figure 4 – Comparison of *Nu* along diverging and converging sections, q_w=const

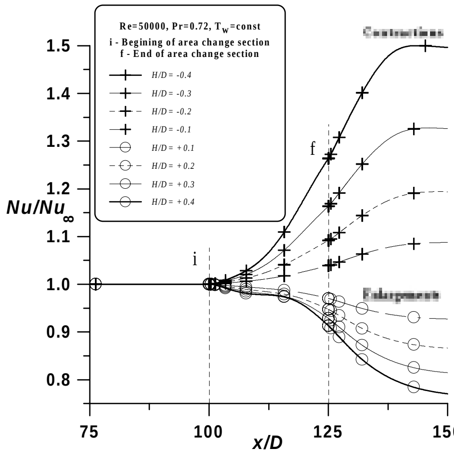

Figure 5 - – Comparison of *Nu* along diverging and converging sections, T_w=const

Determination of the unknown pressure gradient is handled as explained in Patankar (1988). That approach consists in finding the zero of a function representing the discrepancy, at the downstream position, between the *calculated* and *real* duct area. All transport equations for the mean and turbulent fields were solved by means of the marching-forward method of Patankar, 1988.

3. RESULTS AND DISCUSSION

The flow field in the duct shown in Figure 1 was calculated for a long inlet region followed by a converging/diverging duct before another long outlet sector. The objective of this case was to investigate the changes in fully developed profiles occurring past an area change section without the simultaneous hydrodynamic and thermal boundary-layer development at the wall. Then, changes in the mean and turbulent quantities, solely due to duct area variation, could be isolated for analysis. Data used in all cases are summarized in Table 1.

Calculations for the hydrodynamic turbulent field along ducts with varying cross section were discussed in de de Lemos and Milan, 1997, and de Lemos and Braga, 1998, for ducts with sinusoidal and plane walls, respectively. Figures 2-3 summarizes major results therein and shows the behavior of turbulence passing over a variation of area occurring in a duct in the range $100<x/D<125$ (see Figure 1 and Table 1). The figures present the non-dimensional turbulent kinetic energy along a sinusoidal wall duct and at two radial positions, one close to the wall (y/R=0.85) and the other at the centerline (y/R=0.0). It is interesting to note that, within enlargements, Figures 2-3 indicate that an increase in k/U^{*2} takes place across the entire cross section. Even though the mean flow is decelerating, enhancement of turbulent transfer due to steep velocity gradients across the flow indicates that a greater portion of mean kinetic energy is feeding turbulence. An opposite trend, for contracting ducts, is also shown in the figures.

Accelerating flow tend to flatten velocity profiles decreasing turbulence production rates leading, eventually, to relaminarization phenomenon. Ultimately, in a contraction, the mean field acquires more kinetic energy but a lower fraction is made available for generating turbulence. These results are in complete agreement with measurements compiled by Spencer *et al*, 1995.

Corresponding results for the thermal field, calculated with data of Table 1, are shown in Figures 4 and 5 for q_w and T_w constant, respectively. The Nusselt number is calculated finding first the bulk temperature T_b, the film coefficient h and then Nu with the help of the

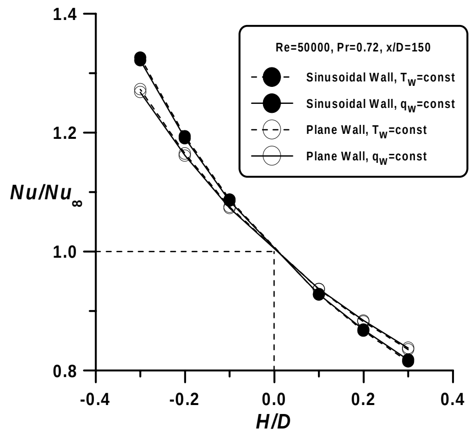

Figure 6 – Effect of contractions/expansions on Nusselt number for plane and sinusoidal duct shape

expressions,

$$T_b = \frac{1}{\dot{m}} \int_A \rho u T dA; \quad h = q_w (T_w - T_b); \quad Nu = hD/k \tag{9}$$

Both Figures show that within contractions, accelerated flow induces a higher *Re* causing an enhancement on the magnitude of turbulent heat transfer through the wall. On the other hand, for duct enlargements, lower speed flow reduces Nusselt numbers being both trends in coherence with the overall correlation of the form $\mathrm{Nu} = \mathrm{Re}^n \, \mathrm{Pr}^m$.

When comparing Figures 2-3 with Figures 4 and 5 *dissimilarity* between Nusselt number and turbulent kinetic energy seems apparent. In the first case (Figures 2-3), acceleration on the flow damps turbulence but, on the other hand, it enhances Nusselt number (Figures 4-5).

Likewise, for flow within duct expansions, there seems to be an enhancement of turbulent momentum transfer whereas heat crosses the wall layers at a lower rate. Therefore, along contractions, while turbulence quantities are decreasing, the heat transfer coefficient increases. Figure 6 summarizes the changes in *Nu* calculated at the exit of the long duct cases (*x/D*=150). Plane wall values are taken from de Lemos and Braga, 1999b, and show a slight dependence on wall duct geometry and nearly no influence of applied boundary condition, as expected.

These results are interesting since, usually, the two flow properties presenting a **dissimilar** behavior, namely the overall levels of turbulent kinetic energy and turbulent Nusselt number are, at a first glance, expected to be **similar**. Finally, one should mention that computations herein are intended to contribute to the preliminary design phase of enginering equipment.

4. CONCLUDING REMARKS

This paper presented computations with the standard *k*-*ε* model for simulation of confined isothermal flow in ducts of varying cross-section. Diverging and converging ducts were calculated showing different or *dissimilar* behavior for Nusselt number and turbulent kinetic energy. In general, accelerated flows in a convergent duct reduce turbulence level even though *Nu* increases by a fairly amount. The opposing trend is observed in expanding passages (decelerating flow). The results herein are expected to contribute to the design and analysis of engineering equipment involving concentric turbulent jets. Potential application of this study may include heat exchanger design and analysis.

5. ACKNOWLEDGMENTS

The authors are thankful to CNPq, Brazil, for their financial support during the course of this research.

6. REFERENCES

Braga, E.J., de Lemos, M.J.S., 1999a, NUMERICAL ANALYSIS OF COAXIAL TURBULENT JETS IN DIFFUSERS AND CONTRACTIONS, *COBEM99 - 13th Braz. Cong. Mech Eng*., Águas de Lindóia, São Paulo, Brazil, Nov. 22-26.

Buresti, G.; Petagna, P.; Talamelli, 1998, A., EXPERIMENTAL INVESTIGATION ON THE TURBULENT NEAR-FIELD OF COAXIAL JETS, *Exp. Th. Fluid Sci.*, v 17, n. 1-2, p. 18-26.

de Lemos, M.J.S., Braga, E.J., 1998, NUMERICAL INVESTIGATION OF TURBULENT DUCT FLOW THROUGH GRADUAL ENLARGEMENTS AND CONTRACTIONS, ASME-FED-vol.245, ISBN: 0-7918-1950-7, *Proc. of FEDSM99* Washington, D.C., USA, June 21-25.

de Lemos, M.J.S., Braga, E.J., 1999b, CHARACTERISTICS OF TURBULENT HEAT TRANSFER IN COAXIAL JETS THROUGH GRADUAL ENLARGEMENTS AND CONTRACTIONS, Paper NHTC-0165, *33rd National Heat Transfer Conference*, Albuquerque, New Mexico, USA, August 15-17.

de Lemos, M.J.S., Milan, A., 1997, MIXING OF CONFINED COAXIAL TURBULENT JETS IN DUCTS OF VARYING CROSS SECTION, *CD-ROM of COBEM97 – 12$^{th.}$ Braz. Cong. Mech. Eng*., Bauru, São Paulo, Brazil, Dec. 8-12.

Jones, W.P., Launder, B.E., 1972, THE PREDICTION OF LAMINARIZATION WITH A TWO-EQUATION MODEL OF TURBULENCE, *Int. J. Heat & Mass Transfer*, vol. 15, pp. 301-314.

Kader, B.A. , Yaglom, A.M., 1972, HEAT AND MASS TRANSFER LAWS FOR FULLY TURBULENT WALL FLOWS, *Int. J. Heat & Mass Transf.*, vol. 15, pp. 2329-2351.

Launder, B.E., Spalding, D.B., 1972, LECTURES IN MATHEMATICAL MODELS OF TURBULENCE, Academic Press, New York.

Launder, B.E., Spalding, D.B., 1974, THE NUMERICAL COMPUTATION OF TURBULENT FLOWS, *Comp. Math. App. Mech. Eng.*, vol. 3, pp. 269-289

Matsumoto, E., de Lemos, M.J.S., 1990, M.J.S., DEVELOPMENT OF AN AXI-SYMMETRIC MIXING LAYER IN A DUCT OF CONSTANT CROSS SECTION, *Proc. of 3rd Braz. Therm. Sci. Meet.*, vol. I, pp. 381-385, Itapema, Brazil, Dec. 10-12.

Park, C.J.; Chen, L.D., 1989, EXPERIMENTAL INVESTIGATION OF CONFINED TURBULENT JETS. PART I. SINGLE-PHASE DATA, *AIAA Journal*, v. 27, n. 11 p. 1506-1510.

Patankar, S.V., 1980, NUMERICAL HEAT TRANSFER AND FLUID FLOW, Mc-Graw Hill.

Patankar, S.V., 1988, PARABOLIC SYSTEMS, Chapter 2 of HANDBOOK OF NUMERICAL HEAT TRANSFER, Rohsenow ed., John Wiley & Sons, New York.

Patankar, S.V., Spalding, D.B., 1972, A CALCULATION PROCEDURE FOR HEAT, MASS AND MOMENTUM TRANSFER IN THREE-DIMENSIONAL PARABOLIC FLOWS, *Int. J. Heat & Mass Transf.*, vol. 15, pp. 1787-1806.

Sellars, J.R., Tribus, M., Klein, J.S., 1956, *Journal of Heat Transfer - Trans ASME,* vol. 78, pp. 441-448.

Spencer, E.A., Heitor, M.V., Castro, I.P., 1995, INTERCOMPARISON OF MEASUREMENTS AND COMPUTATIONS OF FLOW THROUGH A CONTRACTION AND A DIFFUSER, *Flow Meas. and Instr.,* v. 6, n. 1, p. 3-14.